Scripta Materialia 192 (2021) 120–124

Contents lists available at ScienceDirect

Scripta Materialia

journal homepage: www.elsevier.com/locate/scriptamat

Intrinsic nano-diffusion-couple for studying high temperature diffusion in multi-component superalloys

Yolita M. Eggeler[a,1,2], Dorota Kubacka[a,2], Peter Pichler[b,c], Mingjian Wu[a], Erdmann Spiecker[a,*]

[a] Institute of Micro- and Nanostructure Research (IMN) & Center for Nanoanalysis and Electron Microscopy (CENEM), Friedrich-Alexander-University Erlangen-Nürnberg, Interdisciplinary Center for Nanostructured Films (IZNF), Cauerstraße 3, 91058 Erlangen, Germany
[b] Fraunhofer Institute for Integrated Systems and Device Technology IISB, Schottkystraße 10, 91058 Erlangen, Germany
[c] Chair of Electron Devices, Friedrich-Alexander-University Erlangen-Nürnberg, Cauerstraße 6, 91058 Erlangen, Germany

ARTICLE INFO

Article history:
Received 3 August 2020
Revised 24 September 2020
Accepted 1 October 2020
Available online 19 October 2020

Keywords:
Compositionally complex superalloys
Multi-component diffusion
Solute segregation
In situ TEM
DICTRA simulation

ABSTRACT

We present a new approach for the quantitative study of high-temperature diffusion in compositionally complex superalloys on the nano-scale. As key element, the approach utilizes the γ/γ'-microstructure itself as intrinsic nano-diffusion-couple (NDC). By establishing equilibrium at one temperature followed by annealing at a different temperature, well-defined transient states are generated which are studied using STEM-EDXS. We demonstrate this approach for a multi-component superalloy of CMSX-4 type. The temporal evolution of element concentrations is consistently revealed for γ- and γ'-forming elements and is compared to diffusion simulations based on DICTRA. Excellent agreement is obtained for Ni, Co, and Cr whereas diffusion of Al and, in particular, Re lacks behind in experiment. Finally, it is demonstrated that transient states can also be captured by *in situ* TEM using chip-based heating devices. The NDC approach offers great opportunities for diffusion studies in compositionally complex superalloys and might be extended to other two-phase multi-component systems.

© 2020 Acta Materialia Inc. Published by Elsevier Ltd.
This is an open access article under the CC BY license (http://creativecommons.org/licenses/by/4.0/)

Ni-base superalloys exhibit outstanding high-temperature properties making them uniquely suitable for modern jet engines and power plants. Their superior properties arise from their two-phase microstructure composed of γ'-cubes coherently embedded in a γ-matrix. Industrial superalloys contain many alloying elements in order to improve creep strength, phase stability, and oxidation resistance [1]. During processing and service, diffusion of these elements leads to severe changes in the microstructure. In particular, the creep properties of an alloy are strongly affected by diffusion via processes like dislocation climb [2,3], solute segregation to defects [4–8], and rafting [9,10]. Moreover, diffusion plays a key role during oxidation and formation of stable oxide scales [11]. New interest in multi-component diffusion comes from research in high-entropy alloys (HEA) and compositionally complex alloys, where the impact of multi-element environments on (sluggish) diffusion is still controversially discussed [12–14]. The γ-phase of commercial superalloys itself constitutes a compositionally complex phase providing synergies for research in these two fields [15]. Gaining a fundamental and quantitative understanding of diffusion in the multi-component phases of superalloys is not only interesting from a fundamental point of view but also key to computational alloy design which requires realistic modeling of diffusion and solid databases [16,17]. So far, computer simulations in the field of superalloys largely build on diffusion data obtained from quasi-binary diffusion couples [18]. Diffusion data for elements taking into account realistic multi-element environments, like in the γ- and γ'-phases of commercial superalloys, are rare and experimentally difficult to obtain [19,20].

In the present work, we introduce a new approach for studying high-temperature diffusion which can be applied to compositionally complex superalloys. The γ/γ' microstructure itself provides intrinsic nano-diffusion-couples (NDC) which we exploit in our NDC approach illustrated in Fig. 1. First, the system is equilibrated at a temperature T_1, which is characterized by flat concentration profiles in both phases, γ and γ', with concentrations determined by the elemental partitioning behavior (Fig. 1a). In the next step, the temperature is either decreased to a value $T_2 < T_1$ (Fig. 1b) or increased to a value $T_3 > T_1$ (Fig. 1c). The tran-

* Corresponding author.
E-mail address: erdmann.spiecker@fau.de (E. Spiecker).
[1] Present address: Laboratory for electron microscopy, Karlsruhe Institute of Technology, Wolfgang-Gaede-Str. 1a, 76131 Karlsruhe, Germany
[2] These authors contributed equally to this work.

https://doi.org/10.1016/j.scriptamat.2020.10.002
1359-6462/© 2020 Acta Materialia Inc. Published by Elsevier Ltd. This is an open access article under the CC BY license (http://creativecommons.org/licenses/by/4.0/)

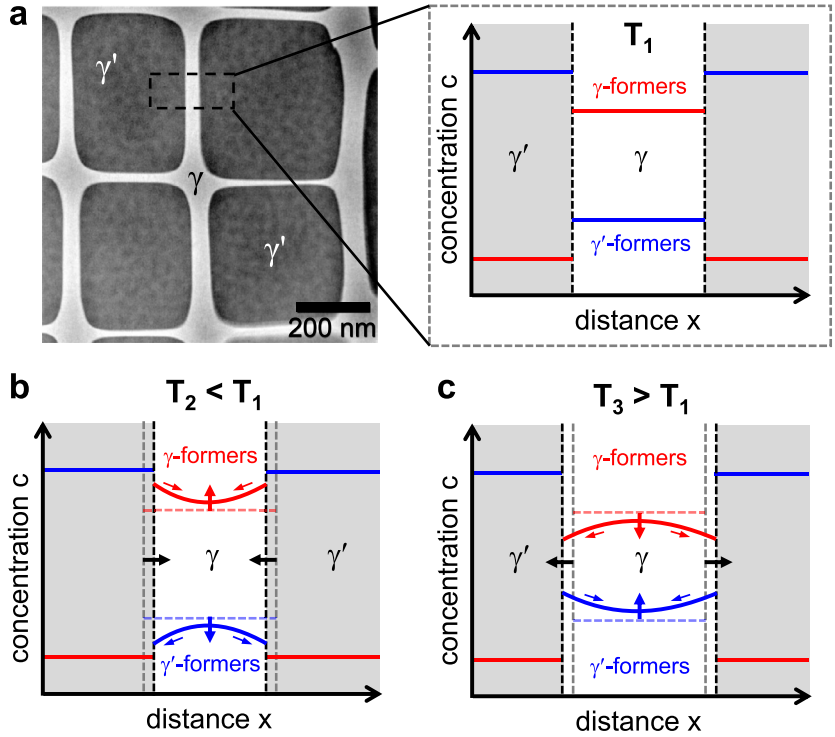

Fig. 1. Illustration of the nano-diffusion-couple (NDC) approach to study interdiffusion of γ- and γ'-forming elements (blue and red) between the two phases. (a) After equilibration at temperature T_1, flat profiles occur in both phases. (b, c) Upon changing the temperature to lower (T_2) or higher (T_3) values transient diffusion profiles develop until the new equilibrium is established. Concurrently the γ'-phase expands (T_2) or contracts (T_3) to establish the new γ' volume fraction. For simplicity, the concentrations in γ' are shown unaltered since the main concentration changes occur in the γ-phase (see text for details). (For interpretation of the references to color in this figure legend, the reader is referred to the web version of this article.)

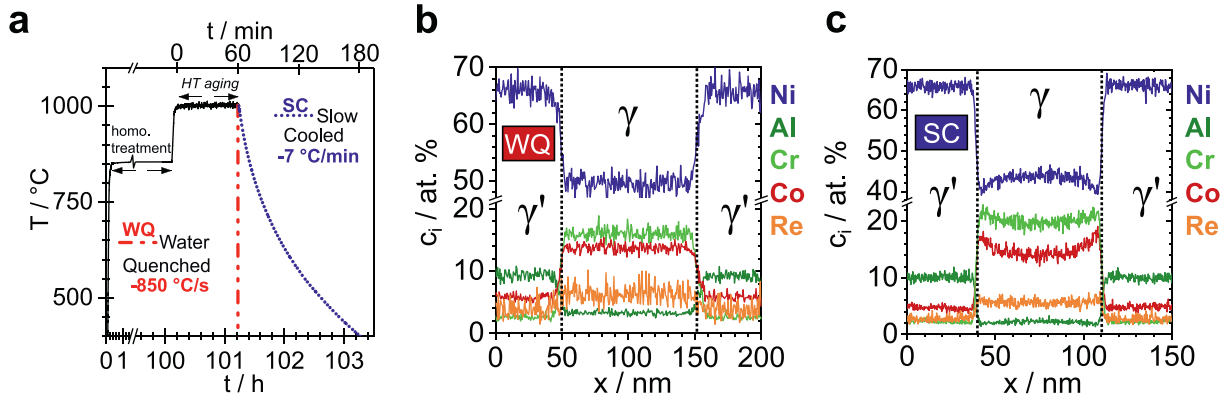

Fig. 2. *Ex situ* fast quenching vs. slow cooling. (a) Temperature-time-profiles. Direct proof of transient states by comparing cross γ-channel concentration profiles after water quenching (WQ) (b) and slow cooling (SC) (c) in a vertical furnace.

sient states are then governed by interdiffusion of the alloying elements and concurrent $\gamma \leftrightarrow \gamma$' phase transformation which together establish the elemental partitioning and γ' volume fraction in the new equilibrium. For $T_2 < T_1$, the γ-formers (blue) diffuse into the γ-channels, whereas the γ'-formers (red) diffuse out. Concurrently, the γ/γ' volume fraction changes, leading to an expansion of the γ'-precipitates and narrowing of the γ-channels. The opposite takes place for $T_3 > T_1$. The idea of the NDC approach is to study high-temperature diffusion by measuring transient states directly on the nanoscale. This can be done either *ex situ* (Figs. 2 and 3) or *in situ* (Fig. 4) using energy-dispersive X-ray spectroscopy in scanning transmission electron microscopy (STEM-EDXS).

Before demonstrating the NDC approach, we consider the expected fluxes of γ- and γ'-formers in further detail. In the schematic drawings of Fig. 1b and c transient profiles and concentration changes are only depicted in the γ-channels, whereas the concentrations in γ' are shown unchanged. In fact, thermodynamic calculations show that the main concentration changes occur in γ, whereas corresponding changes in γ' are typically one order of magnitude smaller (see SI). To understand the consequences of this we consider again the case $T_2 < T_1$ (Fig. 1b). Upon annealing at T_2 the γ'-phase expands and pushes γ-formers (blue) into the narrowing γ-channel. Simultaneously, γ'-formers (red) are sucked (and thus diffuse out) from the γ-channel in order to establish the newly formed γ'-shell around the existing γ'-particle. Much smaller net fluxes of γ- and γ'-formers out of/into the bulk of γ'-precipitates are required to accommodate the minor changes in the γ' equilibrium concentrations (see SI).

We applied the NDC approach to the alloy ERBO/1 which is a Ni-base superalloy of CMSX-4 type [21] and compared the exper-

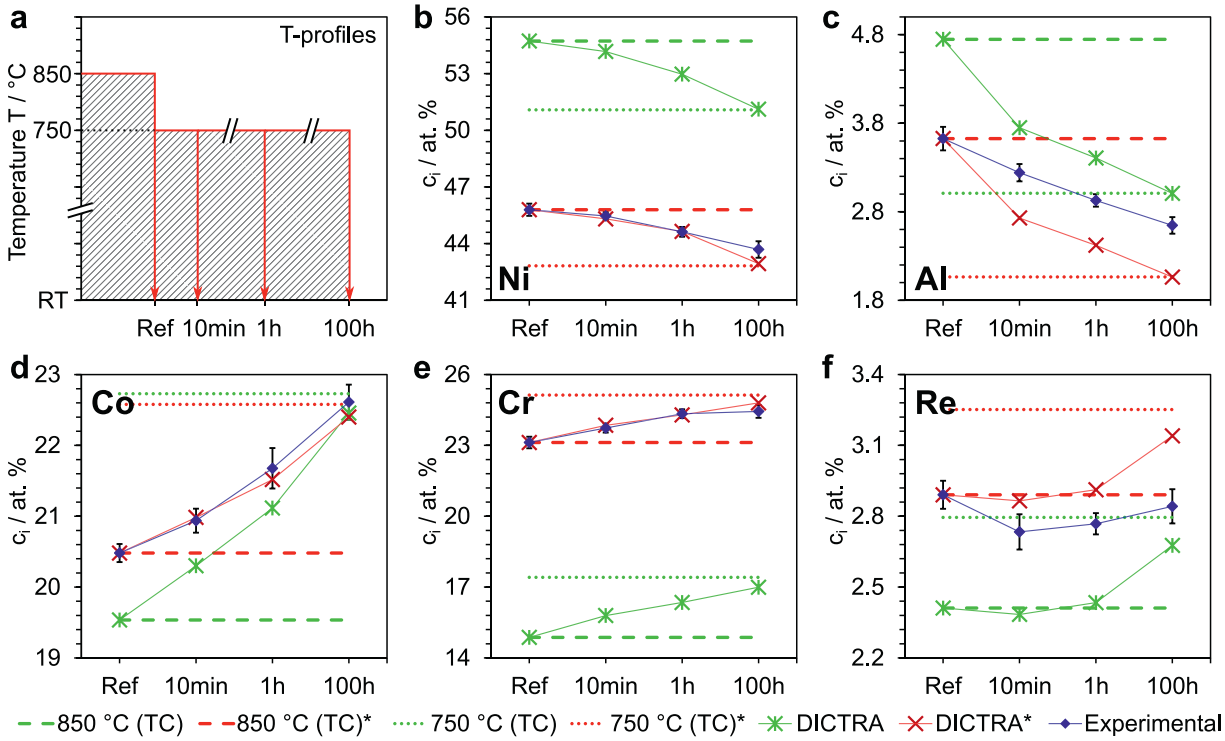

Fig. 3. *Ex situ* heating experiments at 750 °C after equilibration at 850 °C (reference). (a) Temperature-time profiles. (b-f) Comparison between experimental (blue diamonds) and calculated (crosses) total concentration change in the γ-phase for different annealing times. The calculations represented by red crosses were normalized according to the experimental reference concentration. For details see text. (For interpretation of the references to color in this figure legend, the reader is referred to the web version of this article.)

Table 1
Chemical composition of the single-crystal superalloy ERBO/1 in at. %.

Element	Al	Ti	Cr	Co	Ni	Re	Mo	Hf	Ta	W
Nominal chemical composition	12.7	1.3	7.5	9.9	Bal.	1	0.4	0.03	2.2	2.2
Concentration used in simulation	12.7	-	7.5	9.9	Bal.	1	-	-	2.2	2.2

iments with simulations based on Thermo-Calc and DICTRA [22]. Prior to application of the NDC approach all samples were subjected to standard heat treatment, as described in Table 2 of Ref. [21]. The nominal chemical composition of the alloy and the composition used in the DICTRA simulation are listed in Table 1. Due to the complexity of the multicomponent diffusion simulation, the minor alloying elements Ti, Mo and Hf are excluded from the calculation to enable reasonable computation times. Reference states were established in a vertical furnace by isothermal annealing for up to 100 h followed by water quenching. STEM-EDXS measurements were carried out using a double-corrected FEI Titan Themis^3 300 microscope operated at 300 kV and equipped with a Super-X detector. For the isothermal annealing experiment (Fig. 3) solute concentrations in different samples are measured and compared. Therefore, a detailed quantitative EDXS analysis was performed in this case (see SI).

In a first experiment, we compared different quenching rates to demonstrate that (i) high-temperature states can be quenched in and (ii) transient states can be generated and measured on the nanoscale using STEM-EDXS. In order to achieve different quenching rates, we used a vertical furnace, which offers the opportunity to drop the sample from high temperature into a water bath. The corresponding temperature-time profiles have been measured by applying the same quenching procedure to a thermocouple of similar dimension and heat capacity (NiCr/Ni thermocouple shielded by Inconel 600). Fig. 2a shows the temperature-time profiles for the two cooling methods, -850 °C/s by water quenching and -7 °C/min by slow cooling, which were applied to two different ERBO/1 samples. For STEM-EDXS analysis, TEM specimens have been prepared by electropolishing. The diffusion profiles after water quenching appear flat in γ and γ' as shown for Ni, Al, Cr, Co, and Re (Fig. 2b), indicating that the high-temperature state at 1000 °C has been successfully quenched in. In contrast, after slow cooling transient diffusion profiles in γ are clearly detected. In agreement with Fig. 1b, the γ-formers Cr, Co and Re show U-shaped profiles indicating inward diffusion of these elements from γ' whereas inverted profiles are observed for the γ'-formers Ni and Al associated with outward diffusion of these elements from the γ-channel.

After this proof of concept, we moved to *ex situ* isothermal annealing at $T_2 < T_1$ (Fig. 3). The selection of temperatures and annealing times was based on a series of diffusion calculations to yield concentration changes detectable for EDXS and diffusion times that can be covered by the experiment. These calculations were performed using the software PROMIS [23], implementing the diffusion-segregation formalism by You et al. [24], and literature values for the individual diffusion coefficients in γ and γ'. ERBO/1 samples were accordingly equilibrated at 850 °C and subsequently annealed for different times at 750 °C, followed by water quenching (Fig. 3a). We emphasize here that only the reference sample (Ref) was water-quenched from 850 °C. For the other three samples (10 min, 1 h, 100 h) the temperature was directly changed from 850 °C to 750 °C by lowering the sample in the temperature profile of the vertical furnace. This process took only ~10 s, a period which can be neglected compared to the applied anneal-

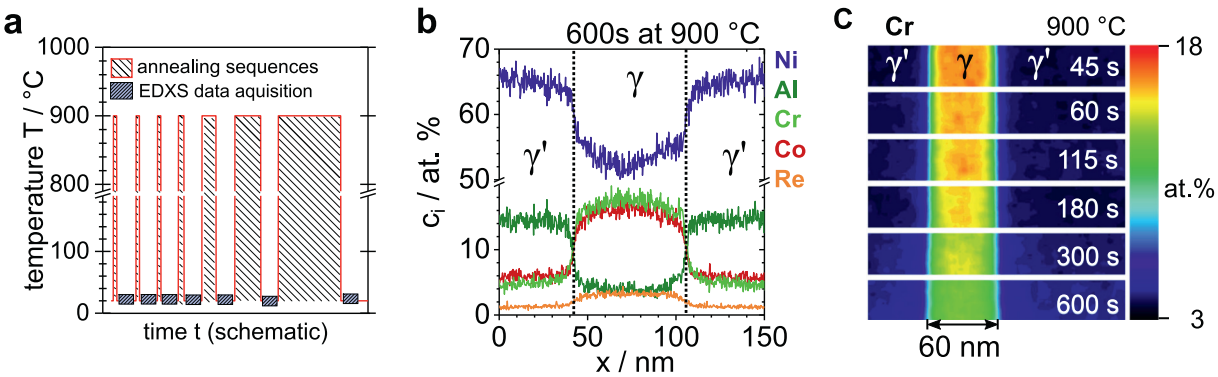

Fig. 4. Interrupted *in situ* heating experiment at 900 °C after equilibration at 850 °C. (a) Schematic temperature-time profile illustrating the experimental procedure. (b) Transient concentration profiles of Ni, Al, Cr, Co, and Re after 600 s at 900 °C. (c) Temporal evolution of Cr concentration in γ and γ'.

ing times at 750 °C. Avoiding quenching in between the annealing steps at T_1 and T_2 (or T_3) is key to the NDC approach. If samples are quenched to RT and heated up again, supersaturation of γ'-formers leads to the formation of tertiary γ'-precipitates in γ-channels during re-heating. As a result, the transient states are affected by the formation and dissolution of tertiary γ' and do not reflect the intrinsic diffusion behavior of the superalloy.

For each of the four samples, at least ten STEM-EDXS concentration maps were acquired from the center of γ-channels and from the adjacent γ'-precipitates, the error bars in the graphs indicate the standard deviation of the data points. Care was taken to measure under identical conditions to enable direct comparison of derived concentrations among the four different samples. In particular, all measurements were taken consistently in interdendritic regions and at the center of γ-channels of approximately the same width using the same sample thickness of 150 nm ± 10 nm, convergence angle, incident beam direction and estimated spatial resolution better than 1 nm (see SI).

According to Fig. 1b and Thermo-Calc data for ERBO/1 (Table S1) the concentrations in γ' are expected to show only minor changes when going from 850 °C to 750 °C. Indeed, no significant concentration changes were detected by EDXS in γ' (Figure S2). In the following, we therefore focus on the concentration changes in the γ-channels and use the concentration values in the channel center to monitor the evolution of the transient states (as indicated by vertical arrows in Fig. 1b). Fig. 3b-f shows the measured concentrations as a function of annealing time for the γ'-formers Ni and Al and the γ-formers Co, Cr, and Re (data points represented by blue diamonds). For all elements except Re the concentrations show a clear and continuous temporal evolution in the expected direction (cf. Fig. 1b), i.e., the concentrations of γ'-formers Ni and Al decrease whereas the concentrations of γ-formers Co and Cr increase. Only the concentration of Re first decreases in the 10 min sample followed by a slight increase at longer annealing times.

The experimental data in Fig. 3 provide quantitative information on how fast the new equilibrium at 750 °C is achieved. This process comprises diffusion of the alloying elements in the multicomponent phases combined with a phase transformation at the interface ($\gamma \leftrightarrow \gamma$'). To compare the results with state-of-the-art simulations we use DICTRA (with mobility database MOBNI5), a versatile software for simulation of diffusion-controlled transformations in multicomponent alloys [22,25]. Using a homogenization model [22], DICTRA allows one to account for the moving γ/γ' interface associated with the change in γ' volume fraction. The boundary conditions for diffusion in the individual phases are determined by assuming local thermodynamic equilibrium at the interface. In the simulation, a one-dimensional planar geometry was assumed. The channel width (49.3 nm) and precipitate size (496 nm) were extracted from the experiment and used as a starting geometry for the simulation.

The concentrations extracted from the DICTRA simulation are shown as green crosses in Fig. 3b-f. As a first result, it can be stated that the temporal evolution of the concentrations in the channel center follow the same trend as in the experiment. In order to see to which extent the new equilibrium concentrations have been reached in the simulation, the green dashed and dotted lines indicate the equilibrium concentrations at 850 °C and 750 °C, respectively, as calculated by Thermo-Calc using the TCNi9 database for 7 elements. According to the DICTRA simulation, Ni and Al have completely reached the new equilibrium concentrations at 750 °C after 100 h of annealing, while Cr and Co have almost reached them. In contrast, the concentration of Re has only increased by ~2/3 of the expected concentration change.

Even though the concentrations in experiment and simulation follow the same trend (Fig. 3b-f), there is a significant offset as well as a difference in the amount of concentration changes for the individual elements. This can be attributed to the fact that only 7 of the 10 elements have been included in the simulation, which affects the equilibrium concentrations, γ' volume fraction and results in less pronounced partitioning. Moreover, deviations may result from the specific data bases used. To enable a direct comparison of experiment and simulation we "normalize" the DICTRA data in the following way. First, we shift the simulation data up or down until the starting concentrations match those of the experiment. Secondly, we re-scale the concentrations of the simulation so that the differences between equilibrium concentrations at 850 °C and 750 °C for the 7-element system fit those of the 10-element system, as derived from Thermo-Calc. The normalized concentrations are shown with red crosses in Fig. 3b-f and are marked with * in the legend. The expected absolute concentration changes for the 10-element system, starting from the first data point, are marked by red dashed and dotted lines.

Normalized data from simulation closely resemble the experimental measurements. An almost perfect match is achieved for Ni, Cr, and Co. In contrast, the experimental concentrations of Al clearly stay behind the simulation indicating a slower diffusion than implemented in DICTRA. An interesting behavior can be observed for the Re concentration, which first decreases at short annealing time (10 min) and then increases towards longer times (1 h, 100 h), in both data sets, simulation and experiment. However, according to the simulation, ~2/3 of the total concentration change should have been accumulated in the center of the γ-channels after annealing for 100 h. In contrast, the experimental data do not show any significant accumulation of Re. This indicates that the diffusion of Re, which is known as a slowly diffusing element, might be even more sluggish than expected.

With the *ex situ* experiments in Figs. 2 and 3, we demonstrated the feasibility of the NDC approach and its rich information content. Using careful annealing and quenching procedures well-defined transient states can be generated. Nanoscale analysis provides quantitative data on the diffusion of alloying elements in the compositionally complex superalloy. One limitation of *ex situ* studies is that the evolution of concentrations cannot be followed in one and the same γ-channel. Rather concentrations in different samples have to be compared requiring statistical analysis and extreme care regarding sample homogeneity (e.g. consistent choice of dendritic or interdendritic regions). We therefore developed an *in situ* approach using a MEMS-based *in situ* TEM heating device, which enables not only ultrafast cooling [26] but also superfast heating. Therefore, interrupted *in situ* annealing experiments become possible, where concentration profiles are measured by EDXS at room temperature (cf. Fig. 4a). In the *in situ* annealing example shown in Fig. 4, the initial equilibration temperature was set to T_1 = 850 °C and *in situ* annealing was performed at T_3 = 900 °C for short times ranging from 45 s to 600 s. Fig. 4b shows the concentration profiles of Ni, Al, Cr, Co, and Re after 600 s. As expected for the case of $T_3 > T_1$ (Fig. 1c), the profiles of the γ'-formers Ni and Al and the γ-formers Cr, Co and Re within the γ-channel reveal a U-shape and inverted U-shape, respectively. The out-diffusion of γ-formers from the γ-channel into γ' is further manifested by the temporal evolution of the Cr concentration shown in Fig. 4c. While the *in situ* approach is highly promising in particular for NDC studies at higher temperatures and short annealing times, quantitative analysis requires a detailed consideration of "thin foil effects" and their potential impact on the measured concentration profiles. Possible thin foil effects include surface oxidation of the TEM sample during high temperature annealing, relaxation of misfit stresses in the thin lamella, and potential contributions of surface diffusion.

In summary, both *ex situ* and *in situ* experiments consistently reveal transient diffusion profiles in accordance with thermodynamic reasoning making us confident that our NDC approach can be applied to obtain quantitative diffusion data for a wide range of superalloys. Applying STEM-EDXS under well-defined experimental conditions enables quantitative analysis of the temporal evolution of the partitioning behavior of all major and some minor alloying elements at the nanoscale. Comparison of the element concentration evolution in *ex situ* experiments with results of multi-component DICTRA simulations shows very good overall agreement, but also reveals significant differences for key γ'- and γ-formers (Al, Re). This clearly indicates the potential of the NDC approach to improve databases of compositionally complex alloys in the future. Dedicated experiments are planned to study cross-diffusion effects, e.g. the impact of a slowly diffusing element on the diffusion of other alloying elements and the overall diffusion kinetics. In general, by evaluating diffusion and diffusional phase transformation in the pristine γ/γ' microstructure of multi-component superalloys our approach can help to elucidate the role of diffusion on high temperature properties, including creep (e.g. Re effect), oxidation behavior or phase stability (e.g. TCP phase formation). Further work is in progress to expand the NDC application to Co-base superalloys and employ other advanced characterization techniques like atom probe tomography.

Declaration of Competing Interest

The authors declare that they have no known competing financial interests or personal relationships that could have appeared to influence the work reported in this paper.

The authors declare the following financial interests/personal relationships which may be considered as potential competing interests.

Acknowledgements

The work was supported by the German Research Foundation (DFG) via project A7 of the Collaborative Research Center SFB/Transregio 103 "From Atoms to Turbine Blades – a Scientific Approach for Developing the Next Generation of Single Crystal Superalloys". The authors also acknowledge financial support by DFG via the Research Training Group GRK 1896 "In situ Microscopy with Electrons, X-rays and Scanning Probes" and usage of instrumentation acquired within the DFG Cluster of Excellence EXC 315 "Engineering of Advanced Materials". They further thank S.G. Fries for the introduction to Thermo-Calc, J. Ågren for supporting DICTRA simulations, N. Karpstein for handling the samples with NanoMilling and M. Lenz for valuable discussions. Y.M.E. acknowledges the support of the Alexander von Humboldt Foundation through the Feodor Lynen fellowship.

Supplementary materials

Supplementary material associated with this article can be found, in the online version, at doi:10.1016/j.scriptamat.2020.10.002.

References

[1] R.C. Reed, Superalloys (2006).
[2] S.M. Hafez Haghighat, G. Eggeler, D. Raabe, Acta Mater. 61 (2013) 3709–3723.
[3] M. Lenz, M. Wu, E. Spiecker, Acta Mater. 191 (2020) 270–279.
[4] T.M. Smith, B.D. Esser, N. Antolin, A. Carlsson, R.E.A. Williams, A. Wessman, T. Hanlon, H.L. Fraser, W. Windl, D.W. McComb, M.J. Mills, Nat. Commun. (2016) 7.
[5] M.S. Titus, R.K. Rhein, P.B. Wells, P.C. Dodge, G.B. Viswanathan, M.J. Mills, A.V. Der Ven, T.M. Pollock, Sci. Adv. 2 (12) (2016).
[6] Y.M. Eggeler, J. Müller, M.S. Titus, A. Suzuki, T.M. Pollock, E. Spiecker, Acta Mater. 113 (2016) 335–349.
[7] D. Barba, E. Alabort, S. Pedrazzini, D.M. Collins, A.J. Wilkinson, P.A.J. Bagot, M.P. Moody, C. Atkinson, A. Jérusalem, R.C. Reed, Acta Mater. 135 (2017) 314–329.
[8] S.K.M. Wu, S.K. Makineni, C.H. Liebscher, G. Dehm, J.R. Mianroodi, P. Shanthraj, B. Svendsen, D. Bürger, G. Eggeler, D. Raabe, B. Gault, Nat. Commun. 11 (389) (2020) 389.
[9] T.M. Pollock, A.S. Argon, Acta Metall. Mater. 42 (6) (1994) 1859–1874.
[10] Y. Tsukada, T. Koyama, Y. Murata, N. Miura, Y. Kondo, Comput. Mater. Sci. 83 (2014) 371–374.
[11] M. Weiser, Y.M. Eggeler, E. Spiecker, S. Virtanen, Corros. Sci. 135 (2018) 78–86.
[12] D. Gaertner, K. Abrahams, J. Kottke, V.A. Esin, I. Steinbach, G. Wilde, S.V. Divinski, Acta Mater. 166 (2019) 357–370.
[13] E.P. George, D. Raabe, R.O. Ritchie, Nat. Rev. Mater. 4 (8) (2019) 515–534.
[14] S. Chen, Q. Li, J. Zhong, F. Xing, L. Zhang, J. Alloys Compd. 791 (2019) 255–264.
[15] J. Chen, X. Zhou, W. Wang, B. Liu, Y. Lv, W. Yang, D. Xu, Y. Liu, J. Alloys Compd. 760 (2018) 15–30.
[16] A. Engström, J. Bratberg, Q. Chen, L. Höglund, P. Mason, Adv. Mater. Res. 278 (2011) 198–203.
[17] A. Chyrkin, A. Epishin, R. Pillai, T. Link, G. Nolze, W.J. Quadakker, J. Phase Equilib. Diffus. 37 (2) (2016) 201–211.
[18] C.E. Campbell, J.C. Zhao, M.F. Henry, J. Phase Equilib. Diffus. 25 (1) (2004) 6–15.
[19] N. Esakkiraja, K. Pandey, A. Dash, A. Paul, Philos. Mag. 99 (18) (2019) 2236–2264.
[20] Y. Chen, R. Prasath Babu, T.J.A. Slater, M. Bai, R. Mitchell, O. Ciuca, M. Preuss, S.J. Haigh, Acta Mater. 110 (2016) 295–305.
[21] A.B. Parsa, P. Wollgramm, H. Buck, C. Somsen, A. Kostka, I. Povstugar, P.-P. Choi, D. Raabe, A. Dlouhy, J. Müller, E. Spiecker, K. Demtroder, J. Schreuer, K. Neuking, G. Eggeler, Adv. Eng. Mater. 17 (2015) 216–230.
[22] H. Larsson, A. Engström, Acta Mater. 54 (9) (2006) 2431–2439.
[23] P. Pichler, W. Jungling, S. Selberherr, E. Guerrero, H.W. Potzl, IEEE Trans. Comput. Aided Des. Integr. Circuits Syst. 32 (1985) 1940–1953.
[24] H.-M. You, U.M. Gösele, T.Y. Tan, J. Appl. Phys. 74 (2461) (1993) 2461–2470.
[25] A. Borgenstam, L. Höglund, J. Ågren, A. Engström, J. Phase Equilib. 21 (3) (2012) 269–280.
[26] F. Niekiel, S.M. Kraschewski, J. Müller, B. Butz, E. Spiecker, Ultramicroscopy 176 (2017) 161–169.